Desalination and Water Treatment
www.deswater.com

doi:10.5004/dwt.2017.20626

72 (2017) 343–353
April

Optimization of chemical modification process of activated carbon surface with iron nanoparticles for efficient vanadium removal: Kinetics, equilibrium and surface complexation modelling

Hakimeh Sharififard, Mansooreh Soleimani*, Farzin Zokaee Ashtiani

Department of Chemical Engineering, Amirkabir University of Technology, No. 424, Hafez Ave., P.O .Box 15875-4413, Tehran, Iran, email: H.sharififard@aut.ac.ir (H. Sharififard), Tel. & Fax +98(21) 66405847, email: Soleimanim@aut.ac.ir (M. Soleimani), Zokaee@aut.ac.ir (F.Z. Ashtiani)

Received 19 August 2016; Accepted 24 February 2017

ABSTRACT

This research deals with the chemical modification of activated carbon surface with the iron functional groups to enhance the adsorption ability. The modification process was optimized and the effects of three factors (temperature, reaction time, and iron concentration) on the removal abilities of iron impregnated activated carbon (I-AC) adsorbents were investigated. The adsorbent prepared at optimum conditions (I-AC-OP) was able to remove about 99.70% of vanadium in 3 h. The iron impregnated adsorbents were characterized using different techniques. Acid-base titrations of activated carbon and I-AC-OP were performed and the surface charge characteristics of adsorbents were determined using FITEQL software. The effects of pH, ionic strength, time and temperature on vanadium removal abilities of adsorbents were evaluated in batch method. Experimental data showed that ionic strength had no influence on vanadium removal. The experimental data of vanadium (V) removal in various pH was modelled by diffuse double layer model (DDLM) using FITEQL software. The results demonstrated that the DDLM is able to fit the removal process in the pH range measured. The kinetic data suggested that chemical adsorption was the controlling step for vanadium removal process, rather than the mass transfer. The maximum adsorption capacity of I-AC-OP for vanadium was 81.96 $mg \cdot g^{-1}$.

Keywords: Activated carbon; Surface modification; Optimization; Surface complexation modeling; Vanadium

1. Introduction

Heavy metals in aqueous mediums, as the main industrial pollutants, are known as hazardous materials due to their toxic effects on human health, and animals. These hazardous materials are non-biodegradable and release to the environment from various industries. One of these metals is vanadium that has been discharged to the environment through different industrial plants. The existence of vanadium in the environment has critical impacts on the human health. An excess amount of vanadium in humans can cause various diseases such as anaemia, cough, emaciation, irritation of mucous membrane, gastrointestinal disturbances and bronchopneumonia. Likewise, excess amount of this hazardous metal in the environment can reduce the productivity of the plants [1–3]. Due to the toxic effects and economic conditions, the removal of vanadium from industrial wastes is essential. The vanadium separation from industrial wastes has been investigated via several processes including precipitation, extraction, membrane process, ion-exchange and adsorption [3–7]. Some of these processes have high capital and operational costs. There are also some problems in disposal of the impure solvents (that contain pollutants) and the residual metal sludge. The results of some research in this area show that the adsorption process can be a satisfying treatment process for the separation of heavy metal ions from aqueous solutions [8].

*Corresponding author.

Because of the unique porous structure, high specific surface area and special chemical structure activated carbons can adsorb many kinds of pollutants from industrial streams, but the selectivity of these adsorbents is low for special pollutant such as vanadium [9,10]. In recent years, the chemical surface modification of activated carbons has attracted extensive interest in order to enhance the ion exchange properties of these adsorbents for selective adsorption of special pollutants. Results of previous investigations indicated that modification of the activated carbon surface can improve the adsorption ability and selectivity of this adsorbent with iron functional groups [11–13]. There are different modification processes that have been suggested for impregnation of iron onto activated carbon surface. In these processes, different iron salts and pre-oxidation agents are used to modify the activated carbon surface under different process conditions [11–16]. Due to reduce the energy and cost of the modification process and suggest an easy process, it is important to study the effects of the main process factors such as temperature, reaction time, iron salt kind and its concentration.

However, there is still a lack of a thorough investigation of the influence of modification process factors on adsorption ability of iron impregnated activated carbon (I-AC) adsorbents [17]. In the previous paper, we modified commercial activated carbon surface by anchorage ferric oxide-hydroxide nanoparticles onto carbon surface and used it for the vanadium removal; but we didn't investigate the effects of modification process factors [18]. Similarly, we used iron sulphate and $KMnO_4$ as pre-oxidation agent [18,19]. To evaluate the effects of iron salt and pre-oxidation agent, we used iron nitrate salt and nitric acid as iron source and pre-oxidation agent, respectively and compared the adsorption ability of this adsorbent with our previous results. The vanadium adsorption process was also modelled using surface complexation method for the first time. Therefore, this study focuses on the following subjects:

- Optimization of the surface modification of activated carbon and synthesis I-AC adsorbents
- Characterization of these adsorbents
- Investigation of the influences of operating parameters on vanadium ion removal
- Modelling of vanadium removal using the surface complexation method
- Study the kinetics, equilibrium and desorption processes

2. Experiments

2.1. Raw materials

The starting extruded activated carbon (ROY 0.8) was purchased from Norit and applied for the surface modification. The starting carbon was denoted as EAC.

2.2. Chemical modification procedure

To chemical modification of EAC surface, 15 g of EAC sample was oxidized as follows:

200 mL nitric acid solution (Merck Co., 63%) and EAC sample were placed into glass round-bottom flask and agitated at 45°C for 3 h. After this time, the pre-oxidized EAC was separated from solution and washed several times with ultra pure water until the pH of washing water would become constant and then, it was dried at 60°C in an air oven overnight.

Each modification test was performed as follows:

0.5 g of pre-oxidized EAC was immersed in 10 mL $Fe(NO_3)_3$ solution with pre-determinediron concentration (mol L^{-1}),and the suspension was shaken at a selected temperature for certain reaction time. After finishing the reaction time, the iron impregnated activated carbon (I-AC) adsorbent was separated from iron-containing solution and washed with ultra pure water several times until the iron content of washing water becomes zero [18]. The adsorbent was oven-dried at 60°C for 1 day.

2.3. Experimental design for modification process

In this study, the effects of three main process factors were studied: iron concentration, reaction time and temperature. The Taguchi method was used for the experimental design and the influences of these factors as well as the optimum process conditions for modification process of activated carbon surface was determined [19,20]. The Taguchi model is one of the most general and widely used experimental design methods that leads to reduce the cost and time [20].

According to Taguchi method, the standard orthogonal array L9, with three columns and nine rows can be used for this process [19]. Table 1 presents the process factors and the settings of these factors for the modification process experiments. In order to validate the predicted results, confirmation experiments were performed twice for optimum process conditions.

The I-AC synthesized samples were applied as adsorbent for vanadium removal according to Table 1 from aqueous solution and removal percentage was selected as the performance characteristic of modification process and the optimum process conditions were determined based on this parameter. Vanadium removal experiments were performed as follows:

Table 1
Arrangement of parameters in L9 orthogonal array

Parameters / Experiment	$Fe(NO_3)_3$ Conc. (M)	Contact time (h)	Temp. (°C)	Removal % (Exp.)	Removal % (Calc.)
1	0.2	5	35	77.81	78.95
2	0.2	14	55	84.64	85.78
3	0.2	24	85	88.95	94.24
4	0.4	5	55	98.00	82.17
5	0.4	14	85	90.30	90.12
6	0.4	24	35	89.95	89.62
7	0.6	5	85	89.10	86.51
8	0.6	14	35	85.00	85.50
9	0.6	24	55	100.00	92.84

0.05 g I-AC was put into contact with 50 mL vanadium solution with an initial concentration of 70 mg L^{-1} at initial pH 4.5 and shaken at 200 rpm at the room temperature for 3 h. After this time, the adsorbent was separated and V (V) concentration in the residual solution was analysed using atomic absorption spectrophotometer (AAS) (Varian AA240, wave length of 318 nm). The percentage of vanadium ions removed by I-AC was calculated and used for analysing using Taguchi method. All the above-mentioned removal experiments were repeated twice times and the average values were reported.

2.4. Characterization of adsorbents

The characterization tests have been done for EAC and I-AC sample that prepared at optimum conditions (I-AC-OP)).

In order to measure the pH_{ZPC} (point of zero charge) of EAC and I-AC-OP, a 50 mL of 0.1 mol L^{-1} NaCl solution was put into glass containers and the initial pH of these solutions was adjusted in the range of 1–12 using 0.1 mol L^{-1} HCl or NaOH solutions (Merck Co.). Then, 0.1 g of adsorbent was added to each container. The containers were agitated for 48 h at 25°C. At the end of this time, filtration was done and the final pH of residual solutions was measured. The point that final pH equals initial pH of NaCl solution, is defined as pH_{ZPC} [8].

The amount of iron, which impregnated onto activated carbon surface, was determined by using X-ray fluorescence (XRF, Unisantis, and XMF-104).

The adsorption-desorption isotherms of N_2 onto EAC and I-AC-OP were measured using an automatic volumetric system (Quantachrome NOVA 1000) and applied to calculate the specific surface area and pore volume of adsorbents according to BET method [21].

Scanning electron micrograph equipped with EDS (SEM-EDS, Tescan) was used to determine the morphology of iron structures that impregnated onto activated surface. The iron distribution and vanadium distribution were analysed by EDS microanalysis and element mapping analysis after adsorption throughout I-AC-OP surface.

The surface chemistry of EAC and I-AC-OP samples was determined by using Fourier transform infrared radiation (Nicolet FT-IR spectrophotometer, NEXUS 670), 4 cm^{-1} resolution, sample/KBr = 1/100 within the range of 400–4000 cm^{-1} wave number.

In order to determine the structure of iron nanoparticle, I-AC-OP sample was analyzed by applying an X-ray diffractometer (XRD, Philips X' Pertdiffractometer, Cu Kα rad).

2.5. Potentiometric titrations for surface complexing modelling

The potentiometric acid-base titration was conducted to determine the surface acidity of EAC and I-AC-OP. Before starting the titration process, 3 g L^{-1} of adsorbent and 50 mL of 0.01 mol L^{-1} $NaClO_4$ as background electrolyte were added to vessel. The suspension was purged with argon gas for 200 min. The initial pH of suspension was adjusted to pH 2.5 by adding 1.5 mol L^{-1} HCl solution. After 1 h, the suspension was slowly titrated with standard NaOH solution (0.05 mol L^{-1}) to pH 11.20. The amount of NaOH solution added during titration process was variable between 0.1 to 0.2 mL. The pH was recorded when the pH variation was less than 0.01 unit per minute. The data sets of pH were used to calculate intrinsic acidity constants versus net consumption of H^+ or OH^{-1} [22].

2.6. Vanadium removal experiments

Effect of pH and ionic strength: In order to investigate the vanadium removal efficiency as a function of initial pH, removal experiments were performed at various initial pH values. In these experiments, initial vanadium concentration, adsorbent dose, agitation speed and temperature were 60 mg L^{-1}, 1 g L^{-1}, 250 rpm and 25°C, respectively. After 3 h, the solution was filtered and vanadium concentration in residual was determined using AAS. To study the effect of ionic strength, the vanadium removal experiments at various pH were conducted without and in the presence of 0.01 mol·L^{-1} $NaClO_4$as background electrolyte.

Kinetics experiments: Kinetics experiments were conducted as follows:

50 mL of vanadium solutions with the initial concentration of 60 mg L^{-1} and initial pH 4.5 were poured into glass Erlenmeyers containing adsorbent (adsorbent dosage = 1 g L^{-1}). The Erlenmeyers were shaken at 200 rpm for the pre-selected times (5, 10, 15, 30, 45, 60, 90, 120, 180, 240 min) at 25°C, 35°C and 45°C. After filtration, the concentration of the vanadium in residual was analysed and the amount of vanadium ions adsorbed by EAC and I-AC-OP, q, was calculated.

Equilibrium experiments: To study the equilibrium isotherms, 0.05 g of adsorbent was put into six Erlenmeyers. Then, 50 mL vanadium ion solution at various initial concentrations (25–50–75–100–150–200 mg L^{-1}) was added to each Erlenmeyer. The initial pH of vanadium solutions was 4.5. The Erlenmeyers were shaken on an orbital shaker incubator at 200 rpm for 24 h at 25°C, 35°C and 45°C. After filtration and analysing the residual solution, the amount of vanadium ions adsorbed by EAC and I-AC-OP, q, was determined.

2.7. Desorption experiments

For investigation of the desorption of vanadium from adsorbents, the adsorbents (EAC and I-AC-OP) were saturated with vanadium ions by contacting 1.2 g of adsorbent with 1 L of vanadium solution (100 mg L^{-1} and pH 4.5) for 48 h. Then, the adsorbents were filtered, washed with distilled water to remove the un-adsorbed vanadium ions and dried in an oven at 70°C overnight.

In desorption experiments, the effects of extractant type (HCl, H_2SO_4, NaOH and Na_2CO_3) and its concentration (0.25–2 mol L^{-1}) were studied. In desorption experiments, 0.1 g of the V(V)-loaded adsorbents was agitated with 50 mL of extractant solution at a speed of 200 rpm at 25°C for 4 h. After filtration, the concentration of vanadium ions was determined in the solution by AAS. The percentage of desorption was calculated by dividing the amount of vanadium ions desorbed by the amount of metal ions adsorbed.

Each desorption run was performed at least two times under identical conditions and the average values were reported.

3. Results and discussion

3.1. Optimizing the modification process

The experimental data obtained for removal of vanadium using I-AC samples is presented in Table 1 and analysed by Taguchi method. The mean effect for each level of the experimental factors is shown in Fig. 1. This figure indicates that the vanadium removal efficiency is increased by increasing the iron concentration, but, at 0.6 mol L^{-1} is slightly decreased. As can be seen in Fig. 1b, an increase in reaction time leads to an increasing vanadium removal efficiency. This may be attributed to increase in the iron content of I-AC samples by increasing the reaction time [19]. By increasing reaction time, the iron molecules have enough time to interact with the functional groups of activated carbon surface and create more active adsorption sites onto I-AC surface. The XRF results showed that the iron content of I-AC samples synthesized at the experimental conditions 1, 4 and 7 in Table 1 were 4.56 wt.%, 7.04 wt.% and 7.30 wt.%, respectively. The initial decrease may be due to an interaction of iron concentration-reaction time and temperature (Fig. 1e, f, g).

The results indicate that the optimum modification conditions are: concentration of iron = 0.4 mol L^{-1}, reaction time = 24 h, and temperature = 55°C. The I-AC adsorbent synthesized at optimum process conditions has the ability to remove about 98.7% the vanadium ions from the aqueous solutions.

Table 2 is the ANOVA results for the modification process. The contribution percentage of error is 7.317, which is not significant [19]. According to the Fisher tables with 90% confidence for vanadium removal by I-AC adsorbents, the significance rate is $F_{0.1, 2, 2} = 9$ [23]. Therefore, the calculated F-value in the ANOVA table is bigger than the standard F-value for iron concentration and temperature factors, and these factors have great effects on the performance characteristic.

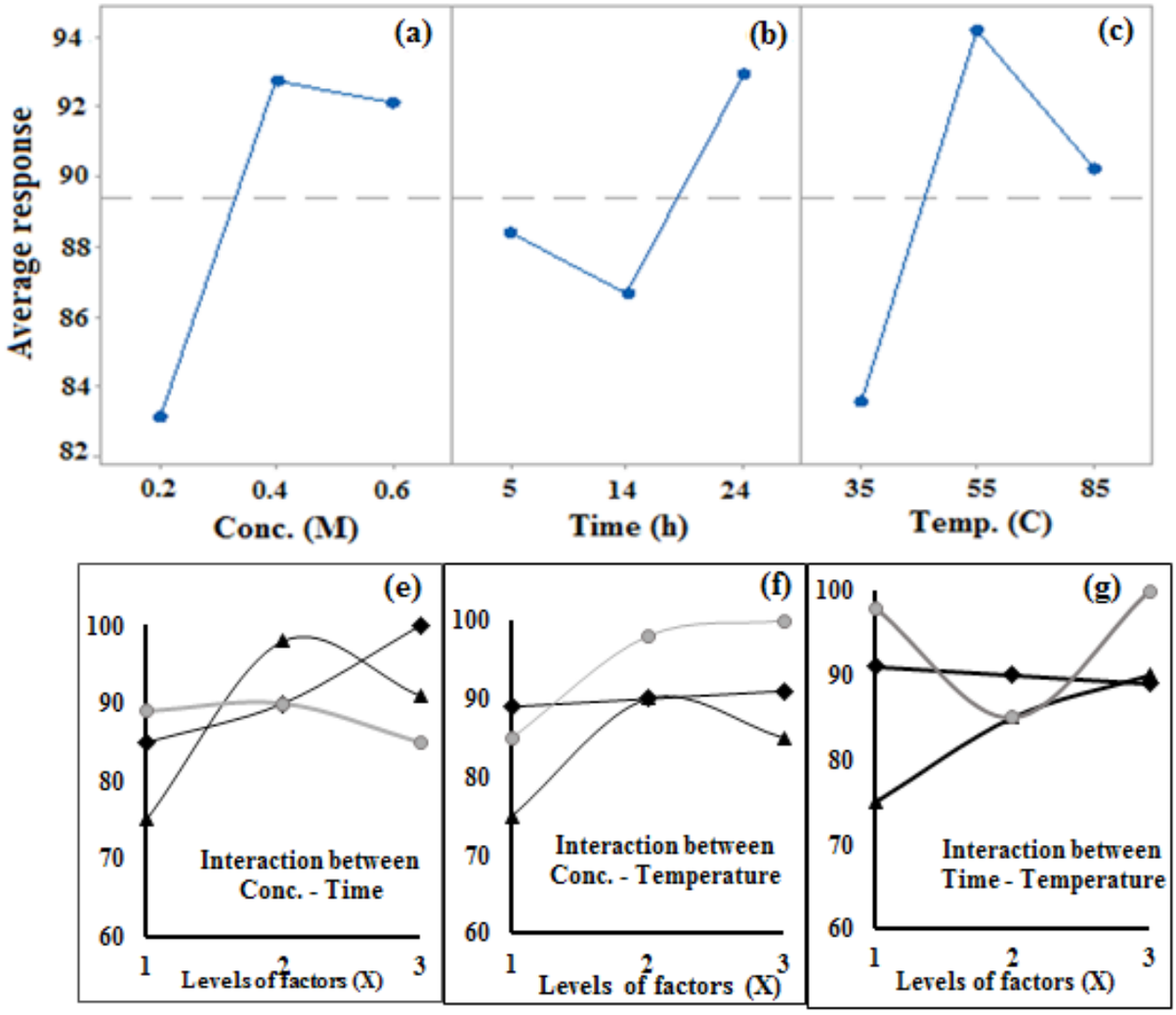

Fig. 1. Effect of process factors on average response: (a) Iron concentration, (b) Reaction time, (c) Temperature, (e) Interaction between Conc. and Time, (f) Interaction between Conc. and Temperature, (g) Interaction between Time and Temperature for modification process.

Table 2
Results of ANOVA table for modification process

Synthesis parameters	Sum of squares	Variance (V)	F-ratio	Contribution percentage
Iron conc. (mol L^{-1})	174.303	87.151	27.777	39.832
Reaction time (h)	63.463	31.731	8.293	13.339
Temp. (C)	172.965	86.482	22.603	39.512
Error	7.651	3.825		7.317
Total	418.384	87.151	27.777	100.000

Taguchi method was used to develop a correlation between performance characteristic and process factors. Eq. (1) describes the relation between vanadium removal % and process factors.

$$R(\%) = 71.5 + 4.9\,\mathrm{Conc.} + 0.51\,\mathrm{Time} + 0.112\,\mathrm{Temp} \quad (1)$$

The predicted values using this equation were reported in Table 1. The results show that this model can describe the modification process efficiently. The standard error of these predicted values was 6.329 that is close to the contribution percentage of error presented in ANOVA Table.

3.2. Characterization of adsorbents

3.2.1. Physical and chemical properties

The amount of iron (wt. %) impregnated onto I-AC-OP surface was 11.64. The iron content of EAC was <0.2 wt. % [18–19]. The pH_{ZPC} of EAC and I-AC-OP samples were 6.50 and 5.05, respectively. The reduction of pH_{ZPC} is the result of the formation of more positive charges on the surface of I-AC-OP. The BET specific surface area and total pore volume of EAC and I-AC-OP were 1062 $m^2\,g^{-1}$, 0.66 mL g^{-1} and 918 $m^2\,g^{-1}$, 0.556 mL g^{-1}, respectively. These results indicate the iron molecules are impregnated onto EAC surface efficiently [18–19].

Fig. 2(a) and (b) show the SEM micrographs of the commercial activated carbon (EAC) and I-AC-OP adsorbent. These micrographs indicate that the iron molecules are impregnated onto EAC surface as nanoparticles, and these nanoparticles have "silvered almonds shape". The size of these nanoparticles ranged from a width of 50 nm to 100 nm and a length of less than 500 nm. Likewise, Fig. 2c and 2d show the EDS and element mapping of I-AC-OP. These figures show the presence of iron on the surface of the adsorbent. Element mapping also shows that the iron is widely distributed on I-AC-OP surface. Fig. 2e and 2f show the presence and distribution of vanadium after adsorption using I-AC-OP by EDS and element mapping analysis.

Fig. 3a shows the FTIR spectra of EAC and I-AC-OP. Table 3 presents the assignments of IR absorption bands [18,24–27]. The data in Table 3 indicate that the iron molecules have chemical interaction with functional groups of activated carbon surface and create new bonds.

The XRD pattern of I-AC-OP sample is demonstrated in Fig. 3b. This figure shows the peaks at 21.3322, 28.9914, 33.1092 and 36.7017 correspond to the standard 00-003-0251. These peaks validate that the FeOOH structures are formed onto EAC surface.

3.2.2. Surface acidity of EAC and INAC-OP:

In Fig. 4a, the acid-base titration data for EAC and I-AC-OP and predicted curves have been illustrated. The total concentration of consumed protons (TOTH) in the titration process was calculated from Eq. (2): [28]:

$$TOTH = \frac{-(V_b - V_{eb1})C_b}{V_0 + V_b} \quad (2)$$

where V_0, V_b, C_b are the initial volume of suspension (mL), the volume of OH^{-1} added at the different titration points (mL) and the concentration of NaOH solution (M), respectively. V_{eb1} (mL), the zero point of titration (ZPT) was obtained from the linear regression analysis of Gran values that were calculated from the following equations and presented in Fig. 5 [28]:

on the acidic side: $G_a = (V_0 + V_{at} + V_b) \times 10^{-pH} \times 100$ (3)

on the basic side: $G_b = (V_0 + V_{at} + V_b) \times 10^{-(13.8-pH)} \times 100$ (4)

where V_{at} presents the total volume of acid solution that was added to the suspension.

Result has shown the amphoteric character of activated carbon which contains one type of amphoteric surface hydroxyl group ≡ SOH, where S is the activated carbon surface [29].

The adsorbent surface was modelled using the single site two-pK model, where the single surface adsorption site may exist on three protonation states: SOH^{2+}, SOH and SO^{-}. The surface protonation and deprotonation reactions can be presented as follows:

$$\equiv \mathrm{SOH} + \mathrm{H}^{+}_{(s)} \rightarrow \equiv \mathrm{SOH}^{+}_{2} \quad (5)$$

$$\equiv \mathrm{SOH} \rightarrow \equiv \mathrm{SO}^{-} + \mathrm{H}^{+}_{(s)} \quad (6)$$

The surface acidity constants for these reactions are defined respectively by:

$$K^{\mathrm{int}}_{S-a1} = \frac{\left\{\equiv SOH^{+}_{2}\right\}}{\left\{\equiv SOH\right\}\left\{H^{+}\right\}_{s}} \quad (7)$$

$$K^{\mathrm{int}}_{S-a2} = \frac{\left\{\equiv SO^{-}\right\}\left\{H^{+}\right\}_{s}}{\left\{\equiv SOH\right\}} \quad (8)$$

where $\{\equiv \mathrm{SOH}\}, \{\mathrm{SOH}^{+}_{2}\}$ and $\{\equiv \mathrm{SO}^{-}\}$ are the concentration of un-protonated, protonated ions and deprotonated amphoteric hydroxyl group, respectively. The titration data were used to determine the surface acidity constants with

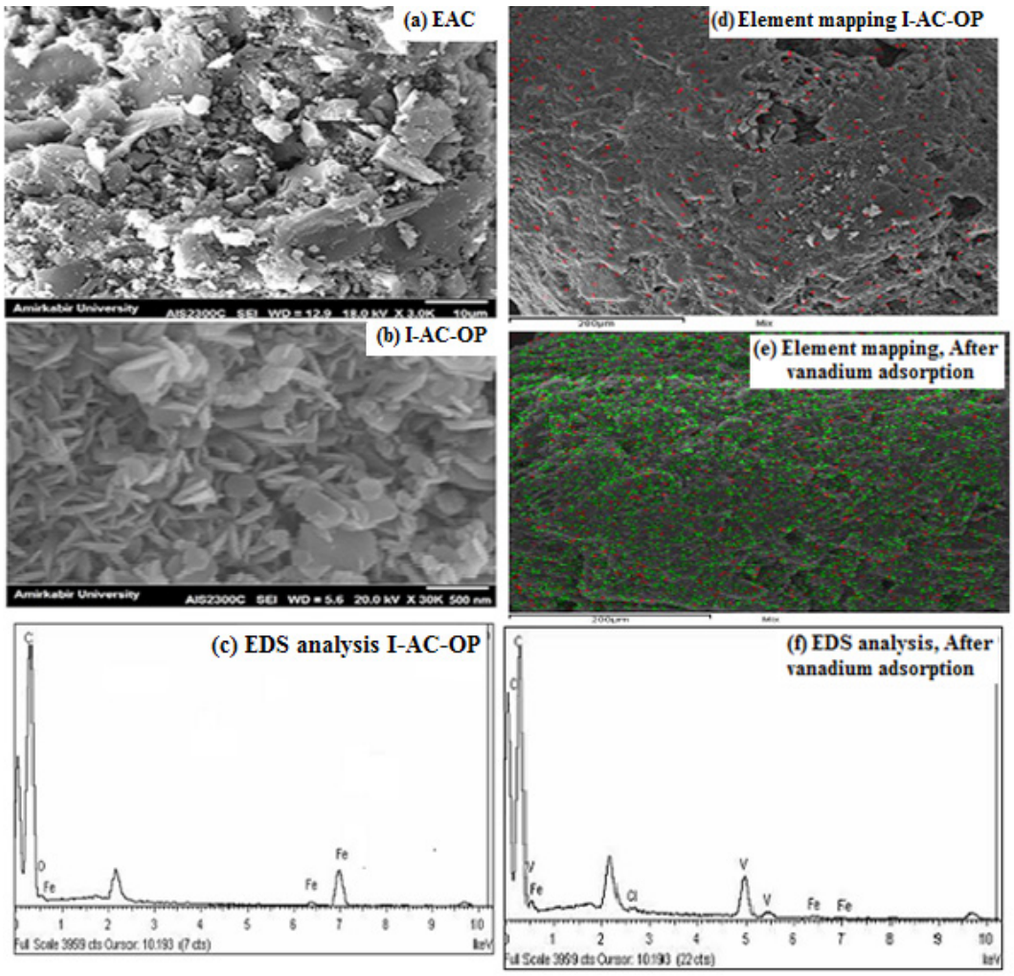

Fig. 2. (a) SEM micrograph of EAC; (b) SEM micrograph of I-AC-OP; (c): EDS analysis of I-AC-OP; (d): Element mapping of I-AC-OP; (e): Element mapping analysis of I-AC-OP after vanadium removal; (f): EDS analysis of I-AC-OP nanocomposite after vanadium adsorption.

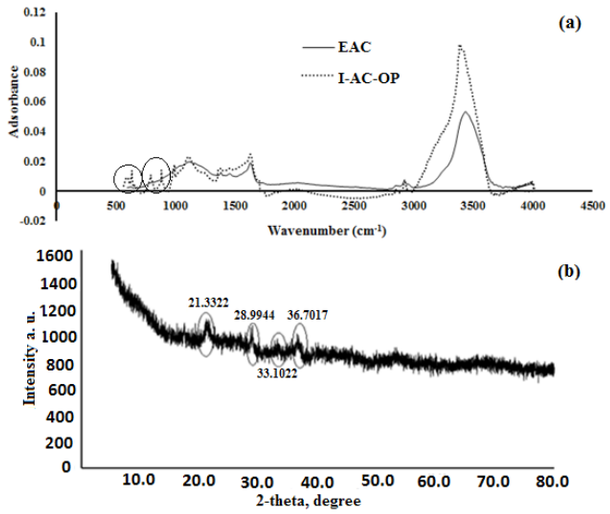

Fig. 3. (a) The FTIR spectra of EAC and I-AC-OP adsorbents; (b) XRD patterns of I-AC-OP composite.

Table 3
Assignments of IR absorption bands for adsorbents [18,24–27]

σ (cm^{-1})	Comments
3434, 3388	Hydroxyl groups (O–H)
2922–2930	C–H aliphatic stretching
2844–2850	–O–CH_3 of the aldehyde group
1630	stretching vibrations of C=O in carbonyl, lactone and carboxyl groups
1455	stretching of C–O or O–H deformation in carboxylic acids
638	Formation of C–O–Fe bonds
790–880	Formation of Fe-O band

the diffuse double layer model (DDLM) using FITEQL v. 4.0 code [30]. The results of the modelling are presented in Table 4. The surface speciation diagram of the surface sites is displayed in Fig. 4b as a function of pH (concentration of surface sites versus pH). Based on the WSOS/DF (weighted

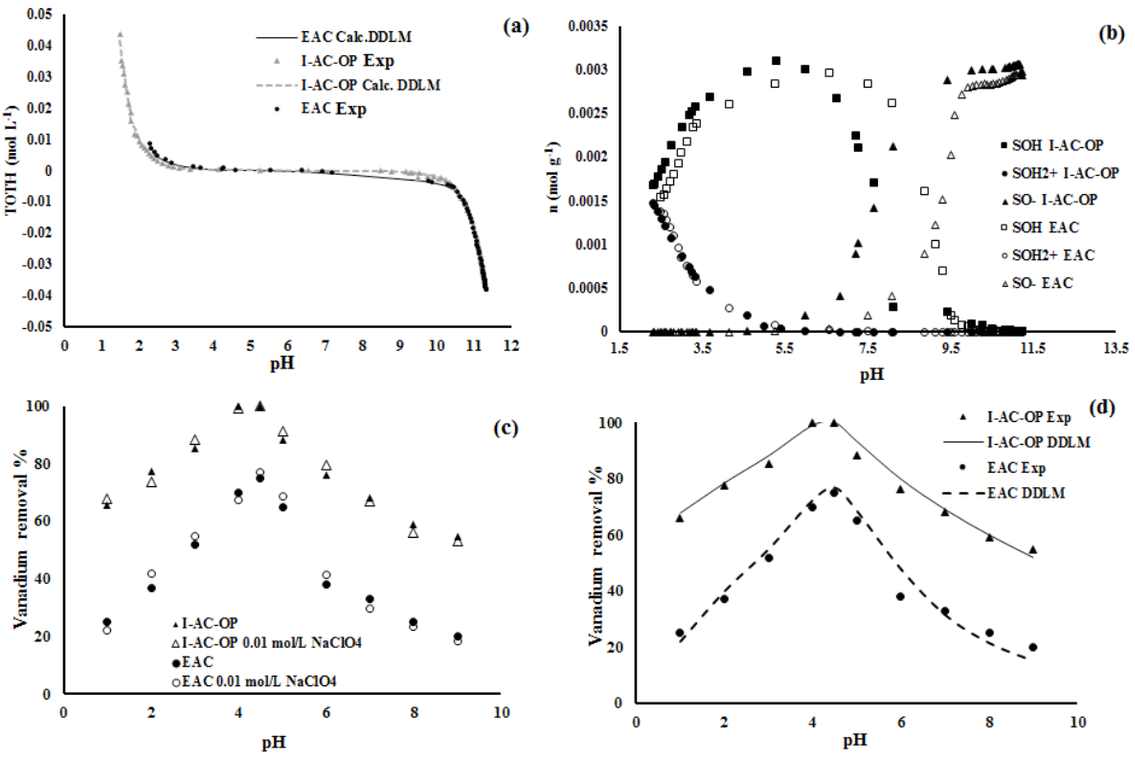

Fig. 4. (a) Acid-base titration diagrams, (b) Surface speciation repartition diagram of adsorbents surface sites as a function of pH, (c) Effect of Ionic strength on vanadium removal, (d) Effect of initial pH on vanadium removal (Points: experimental data; lines: DDLM model predictions).

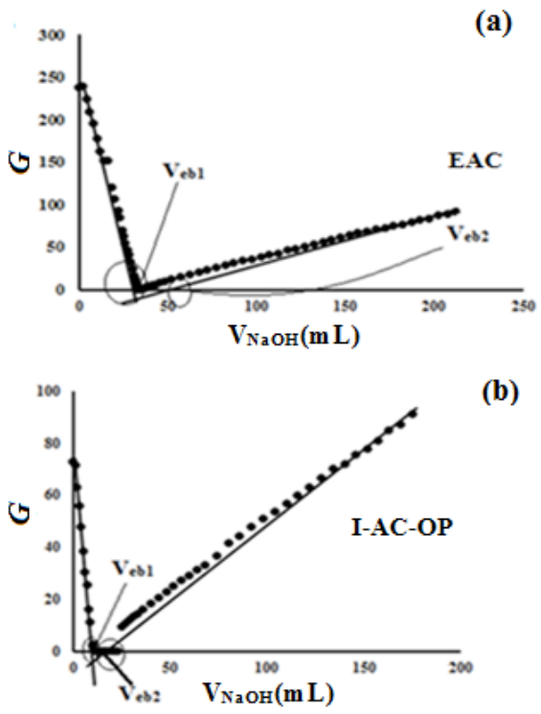

Fig. 5. Gran plots of EAC and I-AC-OP adsorbents.

Table 4
Surface complexation modelling constants and site concentration

Parameters	EAC	I-AC-OP
Intrinsic acidity constants and site concentration		
$\log K^{int}_{S-a1}$	4.273	3.085
$\log K^{int}_{S-a2}$	–8.891	–7.027
Surface site density (mol g^{-1})	3.14×10^{-3}	2.97×10^{-3}
WSOS/DF	13.20	8.98
Surface complexation constants for vanadium adsorption		
Log K_1	2.515	4.831
Log K_2	7.810	19.263
Log K_3	3.671	5.782
WSOS/DF	14.10	10.71

sum of squares of residuals divided by the degree of freedom) parameter values in the range of 0–20, there is a good fitting of experimental data with DDLM model [28]. The WSOS/DF presented in Table 4 indicates that DDLM model provided a good description of surface charge characteristics of I-AC-OP and EAC.

The following equation can been used to calculate the pH_{ZPC} according to acidity constants [28]:

$$\frac{\left|\log K_{S-a1}^{\text{int}}\right| + \left|\log K_{S-a2}^{\text{int}}\right|}{2} = pH_{ZPC} \quad (9)$$

Based on Eq. (9), pH_{ZPC} was obtained 5.06 and 6.58 for I-AC-OP and EAC, respectively. These values are very close to the experimental values (Section 3.2.1).

3.3. Vanadium removal

3.3.1. Effect of initial pH and ionic strength

Fig. 4c presents the experimental data of vanadium removal at two values of ionic strength (zero and 0.01 mol L^{-1}). These data show that the ionic strength has no effect on vanadium removal and it can be suggested that the inner-sphere surface complexation dominates vanadium removal on I-AC-OP and EAC [22]. Other researchers found that vanadium (V) adsorbs onto activated alumina by forming inner-sphere complexes [31].

Fig. 4d shows the effect of initial pH on vanadium removal efficiency of EAC and I-AC-OP. The pH of solution affects the surface charge of adsorbent and the chemical species of adsorbate. The distribution diagram of vanadium species at various pH was evaluated by using FITEQL v4.0 code. According to FITEQL software results, the vanadium exists in the solution as cation (VO_2^+) species at initial pH < 3, and at 4 < initial pH < 11, this metal exists as anionic species ($VO_2(OH)_2^{-1}$ and $VO_3(OH)^{2-}$). The removal efficiency first increased by increasing initial pH (1–4), and then decreased (4.5–9). The pH_{ZPC} of adsorbents was 6.50 and 5.05. The low vanadium removal efficiency at pH < 3 is due to the repulsion between vanadium cations and the positive surface of adsorbents. At higher pH (3.5 < pH < 5), the chemical species of vanadium are anions and can be adsorbed by the positive surface of EAC and I-AC-OP. At pH > 5.5, the surface of adsorbents has a negative charge and therefore, the vanadium removal is decreased [25].

3.3.2 Modelling of Vanadium ion removal using surface complexation method

Vanadium (V) removal data were fitted with DDLM using FITEQL 4.0. Based on the distribution of vanadium species in aqueous solution (Figure has not been shown), the main species of vanadium are VO_2^+ at pH < 3 and $VO_2(OH)_2^-$ and $VO_3(OH)^{2-}$ at 4 < pH < 11. Therefore, the removal data were optimized to simplify their removal processes throughout a wide pH range. The main adsorption reactions can be described by:

$$\equiv SOH + VO_2^+ = SOVO_2^\circ + H^+ \qquad K_1 \quad (10)$$

$$\equiv SOH_2^+ + VO_2(OH)_2^- = SOH_2VO_3^\circ + H_2O \qquad K_2 \quad (11)$$

$$\equiv SOH_2^+ + VO_3(OH)^{2-} = SOVO_2(OH)^{-1} + H_2O \qquad K_3 \quad (12)$$

The log *K* values of Eqs. (10), (11) and (12) are obtained by the best fitting of vanadium removal on I-AC-OP and EAC (Table 4). The calculated curves in Fig. 4d show that DDLM can fit the experimental removal data well. The higher Log *K* values prove higher vanadium removal capacity of I-AC-OP in comparison with EAC.

3.3.3. Adsorption equilibrium

In order to understand the adsorption process clearer, the available equilibrium data were fitted using the Langmuir and Freundlich isotherms. The isotherm equation, isotherm parameters and regression coefficient (R^2) for these isotherms are reported in Table 5. The comparison among the regression coefficients indicates that the Freundlich isotherm can describe the experimental data well. The results of Table 5 suggest that vanadium adsorption on EAC and I-AC-OP takes place as a heterogeneous process. As reported in Table 5, the maximum adsorption capacity of I-AC-OP is 81.96 mg g^{-1} that is higher than that of EAC, and it is as a results of impregnation of iron functional groups with positive charges onto EAC surface [18–19]. The adsorption capacity of I-AC-OP is comparable with the adsorption capacities of other adsorbents for vanadium such as chitosan derivation (12.22 mg g^{-1}), $ZnCl_2$ modified activated carbon (24.90 mg g^{-1}), Fe (III)/Cr (III) hydroxide waste (11.43 mg g^{-1}), Zr (IV)-loaded orange juice residue (51.9 mg g^{-1}), PGTFS–$NH_3^+Cl^-$ (51.98 mg g^{-1}), and polypyrrole coated magnetize d natural zeolite (65.05 mg g^{-1}) [3,32–36].

Our results show that the vanadium adsorption capacity of iron impregnated adsorbent that was synthesized using iron nitrate as iron source and nitric acid as pre-oxidation agent is lower than that adsorbent which was synthesized using iron sulphate and $KMnO_4$ [18,19].

Table 5
Constant parameters and regression coefficients for Langmuir and Freundlich isotherms (C_0 = 25–200 mg L^{-1}, m = 1 g L^{-1}, V = 50 mL)

Isotherm	Parameter	Adsorbent	
		EAC	I-AC-OP
Langmuir $\left(\frac{1}{q_e} = \frac{1}{q_{\max} K_L} \cdot \frac{1}{C_e} + \frac{1}{q_{\max}}\right)$	K_L (L mg^{-1})	0.076	0.174
	q_{max} (mg g^{-1})	37.780	81.967
	R^2	0.940	0.950
Freundlich $\left(\log q_e = \frac{1}{n}\log C_e + \log K_f\right)$	K_f	5.220	26.668
	n	2.280	4.545
	R^2	0.990	0.970

This difference can be related to the difference of chemical activity and ionic radius of iron source and pre-oxidation agent.

3.3.4. Kinetic and activation parameters

The adsorption kinetics of vanadium onto EAC and I-AC-OP were investigated by three common models, namely pseudo-first-order model, pseudo-second-order model and intra particle diffusion model.

The pseudo-first-order model assumes that the limiting step of the adsorption process is the physical interaction between adsorbate molecules (vanadium ions) and adsorbent active sites, and that this interaction can be kinetically described by a first order kinetic equation with no role played by liquid–solid and intra particle diffusion. If this model is appropriate, then the adsorption kinetics can be described by the following equation:

$$q_t = q_e\left(1 - e^{k_1 t}\right) \tag{13}$$

where t is the time (min), q_e and q_t are the amount of vanadium adsorbed at equilibrium and at time t (mg g^{-1}), respectively, and k_1 is the rate constant for the adsorption (pseudo) reaction (min^{-1}).

The experimental data were also analyzed by the pseudo–second–order model, which once again assumes that the overall process is limited by the adsorbent–adsorbate interaction (chemical), but then assumes that this can be described by a second order kinetic equation. In this case, the adsorption kinetics can be described by the following equation:

$$\frac{t}{q_t} = \frac{1}{k_2 q_e^2} + \frac{t}{q_e} \tag{14}$$

in which k_2 (g mg^{-1} min^{-1}) is the rate constant for the adsorption (pseudo) reaction.

Eventually, the possibility that adsorption process is controlled by intra particle diffusion was taken into account. If this is the case, then the adsorption kinetics can be described by the Morris–Weber model [8] according to which it is:

$$q_t = k_{id} t^{1/2} + \theta. \tag{15}$$

in which k_{id} is the intra particle diffusion rate constant, and θ is a constant, the value of which depends on the role played by external (fluid–solid) mass transfer.

The kinetic data were illustrated in Fig. 6 relative to vanadium removal using EAC and I-AC-OP at three different temperatures. Parameters and R^2 values for these models are reported in Table 6. The R^2 values and the comparison between $q_{e,cal}$ and $q_{e,exp}$ indicate that experimental results are much better interpreted by the pseudo-second-order model than by the other models taken into account. This suggests that vanadium adsorption on EAC and INAC-OP is controlled by chemical reaction and can be described by a second order kinetic equation in particular, with a negligible contribution of diffusion, at least in the experimental conditions considered.

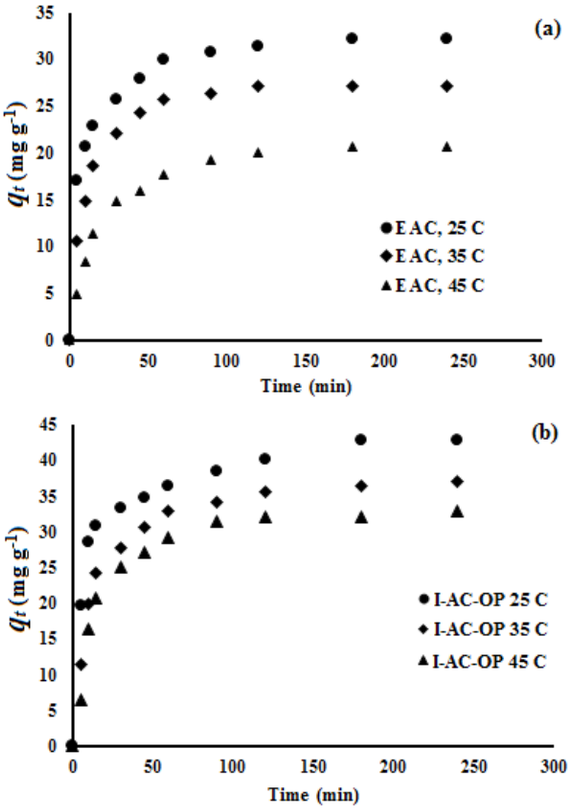

Fig. 6. Amount of vanadium removal as a function of time: (a) EAC; (b) I-AC-OP.

These kinetics data can be used for the calculation of the activation energy according to the Arrhenius equation at different temperatures [37]:

$$\ln k_2 = lnA - \frac{E_a}{RT} \tag{16}$$

where E_a and A are the activation energy (kJ mol^{-1}) and the frequency factor in Arrhenius equation (g gm^{-1} min^{-1}), respectively. The activation energies were –23.91 and –28.04 kJ mol^{-1} for vanadium adsorption onto EAC and I-AC-OP, respectively. The R^2 values for Arrhenius equation were 0.945 and 0.995, respectively. The decrease in the kinetic constant (k_2) with temperature increasing (Table 6) and negative values of activation energy indicate the exothermic nature of vanadium adsorption using EAC and I-AC-OP.

3.3.5. Vanadium desorption

To achieve the practical adsorption, the adsorbate needs to be desorbed and adsorbent reused. The results of desorption experiments are listed in Table 7. According to this table, the best extractant for vanadium ions from two adsorbents was hydrochloric acid 2 M with about 47–50% of vanadium desorption. It can be suggested that in the pH < 2–3, the positive functional groups onto adsorbent surface

Table 6
Kinetics parameters for vanadium adsorption onto EAC and I-AC-OP

Kinetics	Parameter	25°C		35°C		45°C	
Model		EAC	I-AC-OP	EAC	I-AC-OP	EAC	I-AC-OP
$q_{e,exp}$ (mg/g)		32.14	42.80	27.20	37.15	20.71	32.20
Pseudo-first order	k_1	0.026	0.016	0.027	0.021	0.026	0.029
	$q_{e,cal}$	14.25	17.82	12.53	20.75	14.79	22.23
	R^2	0.95	0.91	0.94	0.92	0.937	0.90
Pseudo-second order	k_2	0.0046	0.0053	0.0038	0.0037	0.0025	0.0026
	$q_{e,cal}$	32.89	42.01	29.07	38.70	22.03	34.10
	R^2	0.99	1.00	0.99	0.99	0.99	0.99
Morris–Weber model	k_{id}	1.07	1.47	1.18	1.64	1.11	1.63
	Θ	18.60	23.00	13.61	16.13	6.65	12.51
	R^2	0.81	0.83	0.71	0.83	0.81	0.71

Table 7
The percentages of vanadium desorption from EAC and I-AC-OP

Adsorbent	Extractant	Concentration (mol L^{-1})			
		0.25	0.5	1	2
EAC	HCl	42.0	39.1	32.6	47.5
	H_2SO_4	30.2	31.4	34.3	29.2
	NaOH	32.9	29.6	23.8	17.7
	Na_2CO_3	31.3	29.4	24.5	14.2
I-AC-OP	HCl	31.1	33.2	35.4	51.6
	H_2SO_4	44.4	43.6	42.1	38.7
	NaOH	36.3	33.2	29.5	27.4
	Na_2CO_3	35.1	32.8.	28.9	18.7

repulse the vanadium cations and cause the desorption of vanadium. In accordance with Pearson theory [38], vanadium ions are hard acid groups and have high affinity to hard base groups such as Cl^{-1} ions [18].

4. Conclusions

In this work, commercial extruded activated carbon (EAC) was modified with iron nanoparticles and I-AC adsorbents were synthesized via modification process. Taguchi analysis of experimental data showed that the optimum modification conditions were iron conc. = 0.4 mol L^{-1}, reaction time = 24 h and temperature = 55°C. The vanadium removal with EAC and I-AC-OP (the adsorbent synthesized at optimum conditions) was investigated under various conditions. The results indicated that I-AC-OP was an effective vanadium adsorbent. The maximum vanadium adsorption capacities were 37.87 mg g^{-1} and 81.961 mg g^{-1} for EAC and I-AC-OP, respectively. The concentration of surface sites of adsorbents at different pH was determined using DDLM method with the aid of FITEQL software. The experimental data of vanadium (V) removal has been fitted well versus pH by the diffuse double layer model. The kinetics results showed that the experimental data are much better interpreted by the pseudo-second-order model than by the other models taken into account. The maximum desorption percentage of vanadium ions was obtained when the 2 mol L^{-1} HCl solution was used for EAC and I-AC-OP.

There are different metal ions in industrial waste such as aluminium and zinc. Therefore, it is necessary to investigate the competitive adsorption of vanadium in the presence of other metals.

These batch adsorption data can be used easily in the laboratory for the treatment of small volume of effluents, but less convenient to use on industrial scale, where large volumes of wastewater are continuously generated.

Acknowledgement

The authors sincerely acknowledge the Iran nanotechnology initiative council, Iran, because they received financial support in the form of a research grant [research project No.:61736] from this council. The authors thank Mrs. Tahereh Doostmohammadi for analyzing thesamples by AAS.

References

[1] F.A. Patty, Industrial Hygiene and Toxicology, Interscience Publishers, New York, 1963.
[2] H. Wyers, Some toxic effects of vanadium pentoxide, Br. J. Ind. Med., 3 (1946) 177–182.
[3] A. Padilla-Rodríguez, J.A. Hernández-Viezcas, J.R. Peralta-Videa, G.L. Gardea-Torresdey, O. Perales-Pérez, F.R. Román-Velázquez, Synthesis of protonated chitosan flakes for the removal of vanadium (III, IV and V) oxyanions from aqueous solutions, Microchem. J., 118 (2015) 1–11.
[4] M. Nabavinia, M. Soleimani, A. Kargari, Vanadium recovery from oil refinery sludge using emulsion liquid membrane technique, Int. J. Chem. Environ. Eng., 3 (2012) 149–152.
[5] M. Alibrahim, H. Shlewit, S. Alike, Solvent extraction of vanadium (IV) with di(2-ethylhexyl) phosphoric acid and tributyl phosphate, Chem. Eng. J., 52(1) (2008) 29–33.
[6] A. Dabrowski, Z. Hubicki, P. Podkoscielny, E. Robens, Selective removal of the heavy metal ions from waters and industrial wastewaters by ion-exchange method, Chemosphere, 56 (2004) 91–106.

[7] R. Navarro, J. Guzman, I. Saucedo, J. Revilla, E. Guibal, Vanadium recovery from oil fly ash by leaching, precipitation and solvent extraction processes, Waste Manage., 27 (2007) 425–438.
[8] N. Mehrabi, M. Soleimani, M. Madadi Yeganeh, H. Sharififard, Parameter optimization for nitrate removal from water using activated carbon and composite of activated carbon and Fe_3O_4 nanoparticles, RSC Adv., 5 (2015) 51470–51482.
[9] R. Chand-Bansal, M. Goyal, Activated Carbon Adsorption, CRC Press, Taylor & Francis Groups, Boca Raton, 2005.
[10] H. Marsh, F. Rodriguez-Reinoso, Activated Carbon, Elsevier, New York, 2006.
[11] J.H. Xu, N. Gao, Y. Deng, S. Xia, Nanoscale iron hydroxide-doped granular activated carbon (Fe-GAC) as a sorbent for perchlorate in water, Chem. Eng. J., 222 (2013) 520–526.
[12] A.M. Cooper, K.D. Hristovski, T. Möller, P. Westerhoff, P. Sylvester, The effect of carbon type on arsenic and trichloroethylene removal capabilities of iron (hydr) oxide nanoparticle-impregnated granulated activated carbons, J. Hazard. Mater., 183 (2010) 381–388.
[13] J.A. Arcibar-Orozco, J.R. Rangel-Mendez, T.J. Bandosz, Reactive adsorption of SO_2 on activated carbons with deposited iron nanoparticles, J. Hazard. Mater., 246–247 (2013) 300–309.
[14] H.S. Zhu, J.R. Koduru, K.H. Choo, B. Lee, Activated carbons impregnated with iron oxide nanoparticles for enhanced removal of bisphenol A and natural organic matter, J. Hazard. Mater., 286 (2015) 315–324.
[15] B. Kakavandi, R. Rezaie Kalantary, A. Jonidi Jafari, S. Nasseri, A. Ameri, A. Esrafili, A. Azari, Pb(II) adsorption onto a magnetic composite of activated carbon and superparamagnetic Fe_3O_4 nanoparticles: experimental and modeling study, Clean: Soil Air Water, 43 (2015) 1157–1166.
[16] A. Yurun, Z.O. Kocabas-Atakl, M. Sezen, R. Semiat, Y. Yurun, Fast deposition of porous iron oxide on activated carbon by microwave heating and arsenic (V) removal from water, Chem. Eng. J., 242 (2014) 321–332.
[17] C. Nieto-Delgado, J.R. Rangel-Mendez, Anchorage of iron hydro(oxide) nanoparticles onto activated carbon to remove As(V) from water, Water Res., 46 (2012) 2973–2982.
[18] H. Sharififard, M. Soleimani, Performance comparison of activated carbon and ferric oxide-hydroxide–activated carbon nanocomposite as vanadium (V) ion adsorbents, RSC Adv., 5 (2015) 80650–80660.
[19] H. Sharififard, M. Soleimani, F. Zokaee Ashtiani, Application of nanoscale iron oxide-hydroxide impregnated activated carbon (Fe-AC) as an adsorbent for vanadium recovery from aqueous solutions, Desal. Wat. Treat., 57 (2016) 15714–15723.
[20] D.C. Montgomery, Design and Analysis of Experiments, 3rd ed., Wiley, New York, 1991.
[21] S. Lowell, J.E. Shields, M.A. Thomas, M. Thommes, Characterization of Porous Materials and Powders: Surface Area, Pore Size and Density, Springer, Dordrecht, 2004.
[22] Y. Sun, Q. Wang, C. Chen, X. Tan, X. Wang, Interaction between Eu(III) and graphene oxide nanosheets investigated by batch and extended X-ray absorption fine structure spectroscopy and by modeling techniques, Environ. Sci. Technol., 46 (2012) 6020–6027.
[23] R.A. Fischer, Statistical Methods for Research Workers, Oliver & Boyd, London, 1925.
[24] Z. Al-Qodah, R. Shawabkah, Production and characterization of granular activated carbon from activated sludge, Braz. J. Chem. Eng., 26 (2009) 127–136.
[25] H. Sharififard, F. Zokaee Ashtiani, M. Soleimani, Adsorption of palladium and platinum from aqueous solution by chitosan and activated carbon coated with chitosan, Asia-Pac. J. Chem. Eng., 8 (2013) 384–395.
[26] P. Cambier, Infrared study of goethite of varying crystallinity and particle size: I. interpretation of OH and lattice vibration frequencies, Clay Miner., 21 (1986) 191–200.
[27] Y. Li, C. Zhu, T. Lu, Z. Guo, D. Zhang, J. Ma, S. Zhu, Simple fabrication of a Fe_2O_3/carbon composite for use in a high-performance lithium ion battery, Carbon, 52 (2013) 565–573.
[28] C. Chen, J. Hu, D. Xu, X. Tan, Y. Meng, X. Wang, Surface complexation modeling of Sr(II) and Eu(III) adsorption onto oxidized multiwall carbon nanotubes, J. Colloid Interf. Sci., 323 (2008) 33–41.
[29] K. Kadirvelu, C. Faur-Brasquet, P. Le Cloires, Removal of Cu(II), Pb(II) and Ni(II) by adsorption onto activated carbon cloths, Langmiur, 16 (2000) 8404–8409.
[30] A.L. Herbelin, J.C. Westall, FITEQL 4.0: A Computer Program for Determination of Chemical Equilibrium Constants from Experimental Data. Rep 99–01, Department of Chemistry, Oregon State University, Corvallis, 1999.
[31] T. Su, X. Guan, G. Gu, J. Wang, Adsorption characteristics of As(V), Se(IV), and V(V) onto activated alumina: Effects of pH, surface loading, and ionic strength, J. Colloid Interf. Sci., 326 (2008) 347–353.
[32] C. Namasivayam, D. Sangeetha, Removal and recovery of vanadium (V) by adsorption onto $ZnCl_2$ activated carbon: kinetics and isotherms, Adsorption, 12 (2006) 103–117.
[33] Q. Hu, H. Paudyal, J. Zhao, F. Huo, K. Inoue, H. Liu, Adsorptive recovery of vanadium (V) from chromium (VI)-containing effluent by Zr(IV)-loaded orange juice residue, Chem. Eng. J., 248 (2014) 79–88.
[34] K. Prathap, C. Namasivayam, Adsorption of vanadate (V) on Fe(III)/Cr(III) hydroxide waste, Environ. Chem. Lett., 8 (2010) 363–371.
[35] N.H. Mthombeni, S. Mbakop, A. Ochieng, M.S. Onyango, Vanadium (V) adsorption isotherms and kinetics using polypyrrole coated magnetized natural zeolite, J. Taiwan Inst. Chem. E., 66 (2016) 172–180.
[36] T.S. Anirudhan, P.G. Radhakrishnan, Adsorptive performance of an amine-functionalizedpoly(hydroxyethylmethacrylate)-grafted tamarind fruit shell for vanadium(V)removal from aqueous solutions, Chem. Eng. J., 165 (2010) 142–150.
[37] V.J. Inglezakis, A.A. Zorpas, Heat of adsorption, adsorption energy and activation energy in adsorption and ion exchange systems, Desal. Water Treat., 39 (2012) 149–157.
[38] R.G. Pearson, Hard and soft acids and bases, J. Am. Chem. Soc., 85 (1963) 3533–3539.